



OPEN

## Origami paper analytical assay based on metal complex sensor for rapid determination of blood cyanide concentration in fire survivors

Azarmidokht Sheini<sup>1✉</sup>, Marzieh Dadkhah Aseman<sup>2</sup> & Mohammad Mahdi Bordbar<sup>3</sup>

Cyanide-based blood poisoning can seriously damage fire victims and cause death if not detected quickly. Previous conventional methods require laboratory equipment, which are expensive and increase the duration of the analysis. Here, a simple origami based microfluidic device was introduced for point of need detection of blood cyanide concentration in people involved in fire. The device is made of four layers of paper. Each layer was in the size of 1 × 1 cm folded on each other. In this work, the blood sample was acidified by trichloroacetic acid to separate cyanide from methaemoglobin in the form of HCN gas. The produced gas released into borate buffer to recover free cyanide ions which interacted with the Pt complex ([Pt(*p*-MeC<sub>6</sub>H<sub>4</sub>)<sub>2</sub>(phen)]]) used as a receptor in this study. Optimized conditions were applied to have a suitable interaction causing the color of the receptor to change from yellow to colorless. The color changes were recorded by a smartphone, and the sensor response was calculated by the routine image analysis software. The assay was capable of determining cyanide ions at different concentrations in the range of 1.0 to 100.0 μmol L<sup>-1</sup>. The detection limit of these determination was equal to 0.4 μmol L<sup>-1</sup>. The assay responses were not affected by the interfering species. As a practical analysis, the proposed sensor was applied to determine cyanide ions in the blood sample of 20 studied fire survivors and 10 controls with high accuracy.

Cyanide is one of the toxic substances in the fire smoke<sup>1</sup>. Type of materials, burning temperature and period of fire can influence the amount of cyanide<sup>2</sup>. Humans can be exposed to cyanide contamination through inhalation or skin adsorption of smoke<sup>3</sup>. The inhaled cyanide has high affinity to bind with groups of some proteins and enzymes in tissues and blood such as cytochrome oxidase and methaemoglobin causing hypoxia, respiratory disorders and even death<sup>3</sup>.

In fire occurrence, determination of blood cyanide concentration (BCC) is one of the goals of forensic and medical centers<sup>4–6</sup>. In general, BCC has been analyzed by some popular methods based on electrochemistry and chromatography<sup>7,8</sup>. The techniques represent reliable results, but their experiment procedures require sophisticated instruments, harmful reagents, time-consuming preparations, and skilled experts.

The colorimetric sensors were used as an appropriate alternative for rapid determination of cyanide<sup>9–12</sup>. Among various sensing elements employed in these sensors, metal complexes have been much considered due to having a comfortable preparation method and providing sensitive and selective responses with a simple detection mechanism<sup>13,14</sup>. According to this approach, detection of cyanide was performed using Zn (II) complexes<sup>14,15</sup>, Co (II) complexes<sup>16</sup> and Cu (II) complexes<sup>17–20</sup>.

Recently, square-planar platinum (II) complexes have attracted considerable attention as effective chemical sensors owing to their interesting structures and other colorimetric and luminescence properties<sup>21–23</sup>. They have a high tendency to participate in metal–metal and π–π interactions<sup>22,23</sup>. Therefore, these complexes exhibit high performance in detecting different types of molecules and ions in vapor or liquid phases such as oxygen, pH, carbon dioxide, ammonia, specific metal ions and anions, toxic molecules and biomolecules<sup>24</sup>. In the case of cyanide, Pt exhibits high affinity to this anion and forms a stable Pt-CN complex<sup>25</sup>. The logarithm of the

<sup>1</sup>Department of Mechanical Engineering, Shohadaye Hoveizeh University of Technology, 78986 Susangerd, Iran. <sup>2</sup>Department of Chemistry, Faculty of Sciences, Tarbiat Modares University, 4838 Tehran, Iran. <sup>3</sup>Independent Researcher, Personal Laboratory, 74614 Fasa, Iran. ✉email: noyanchem2019@gmail.com

stability constant for this complex is equal to 40, being higher than that coordinated by copper, nickel, zinc or cobalt<sup>25</sup>. Therefore, it appears that sensor-based Pt complexes have high potential to determine cyanide ions at low concentrations in blood samples and without any interference.

The above sensing applications have some limitations in measurements such as using a difficult sample preparation process prior to BCC determination, needing large amounts of reagents and employing glassware and a complex readout device to monitor the color changes. In addition, it is impossible to use them for in situ analyses<sup>26</sup>.

Paper-based sensors are well-known as feasible tools in analytical chemistry owing to their attractive advantages such as simplicity in preparation, easy use, inexpensive application, compatibility with nature, portability for commercial and point of care analyses<sup>27,28</sup>. Owing to their flexibility, these devices can be designed in origami format<sup>29–32</sup>. The origami based sensor provides a high dimensional flow that makes the sensor includes several analytical operations, such as separation, purification, and pre-concentration before sensing the sample on a single platform<sup>29</sup>. Therefore, the time and volume of reagents required for analysis are significantly reduced. Paper analytical device (PAD) can be combined with different transducers to implement colorimetric, fluorimetric and electrochemical applications<sup>29,33,34</sup>.

Cyanide in blood binds with hemoglobin<sup>1</sup>. By acidification of blood samples, the protein is degraded and separated from cyanide. Under acidic conditions, the released ions are protonated, causing the formation of gaseous hydrogen cyanide (HCN). The gas produced is entered to strong alkaline solution and deprotonated, so that cyanide ions are created<sup>35</sup>. In most of previous studies, Conway cells were used for both separation and diffusion procedures<sup>1</sup>. Although it is an efficient method, it still prolongs the analysis time or uses a large amount of strong acid and base, which is not safe and economical.

In summarize, there are many methods in the literature for the colorimetric determination of cyanide in the blood samples but they are not user-friendly, cost-effective and safe. These method expend a plenty of time for preparation of blood sample, need large volumes of reagents, use fragile glassware, complex instruments and strong acids and bases. These limitations are diminished in the present study by developing a new three-dimensional  $\mu$ PAD based on colorimetric determination of BCC. Unlike the other microfluidic structures used for detection of cyanide, the proposed  $\mu$ PAD is designed on a multilayer paper, which is capable of carrying out the protein degradation, hydrogen cyanide production, and cyanide ion release and identification without using Conway cells. Compared to previous colorimetric techniques, this study used a derivative of platinum (II) complexes, ([Pt(*p*-MeC<sub>6</sub>H<sub>4</sub>)<sub>2</sub>(phen))], which is called as receptor. It has already proven that these complexes have high affinity to cyanide ions, therefore, it is expected that the new sensor has high sensitivity to the low concentrations of cyanide in the blood samples. In this method, we want to use weaker acids and bases to provide a safe assay. The  $\mu$ PAD is fabricated in the size of (1 cm × 1 cm), which can be portable. It seems that this sensor can consume less volume of analyte and reagents. However, the assay should be calibrated under optimal conditions, and its selectivity should be investigated in the presence of other species, so that it can be used to measure cyanide in the blood sample of fire survivors.

## Results and discussions

**Characterization of fabricated  $\mu$ PAD.** The process of pattern designing and fabrication was evaluated by field emission scanning electron microscopy. The SEM images shown in Fig. S2 demonstrate that the bare paper is constructed by interwoven cellulose fibers (Fig. S2b-1). After printing and baking the paper, the ink penetrated into the paper texture and blocked the pores and masked the fibers (Fig. S2b-2). Therefore, the barrier section was resistant to water infiltration. Figure S2c indicates that the Pt complex was homogeneously distributed on the surface of paper.

To confirm that the preparation of the detection zone was repeatable, five individual  $\mu$ PADs were filled by 1.0  $\mu$ L of the receptor. The color intensities for each detection zone were determined and collected in Table S1. The relative standard error (RSD) for these measurements was calculated. The low error values demonstrate that the injection of the receptor was performed in a repeatable process.

**Sensing process.** The injecting sample was entered to  $\mu$ PAD and directed to the acidification layer. In this layer, the cyanide was separated from protein and converted to protonated form HCN. This event occurred by decomposition of protein. The produced gas was followed to gas collection layer and then transferred to alkalization zone. In the alkaline media, gas was deprotonated and the cyanide ions were provided, which were moved to the detection zone and interacted with the Pt complex. Due to interaction, the color of the receptor changed from yellow color to being colorless. Figure 1c and Fig. 1d present the images of the detection zone before and after interaction. This interaction was also investigated by a UV–Vis spectrophotometer. As Fig. S2d shows, the receptor has a maximum peak at 420 nm, which decreases after interaction with cyanide ions, confirming the results of visual detection. On the basis of published reports, it seems that the cyanide ions could replace labile ligands such as Cl<sup>−</sup>, DMSO and SMe<sub>2</sub> on Pt(II) center but the *p*-MeC<sub>6</sub>H<sub>4</sub> or 1,10-phenanthroline ligands in structure of complex A were not replaced with such anion. Probably, the reaction of complex A with cyanide led to formation of the Pt (IV) complex [Pt(*p*-MeC<sub>6</sub>H<sub>4</sub>)<sub>2</sub>(phen)(CN)<sub>2</sub>], (Compound B), by oxidative addition of two cyanide anions onto the Pt(II) center. The chemical reaction equation for cyanide detection is shown in Fig. S1b.

**Optimization.** Different experimental parameters such as concentration of trichloroacetic acid (TCA), type, pH and concentration of buffer, amount of the receptor, number of layers for gas collection and volume of analyte can influence the mechanism of the complex formation between the receptor and the cyanide ion. These parameters should be optimized to have a stable complex and a convenient response for the proposed assay.

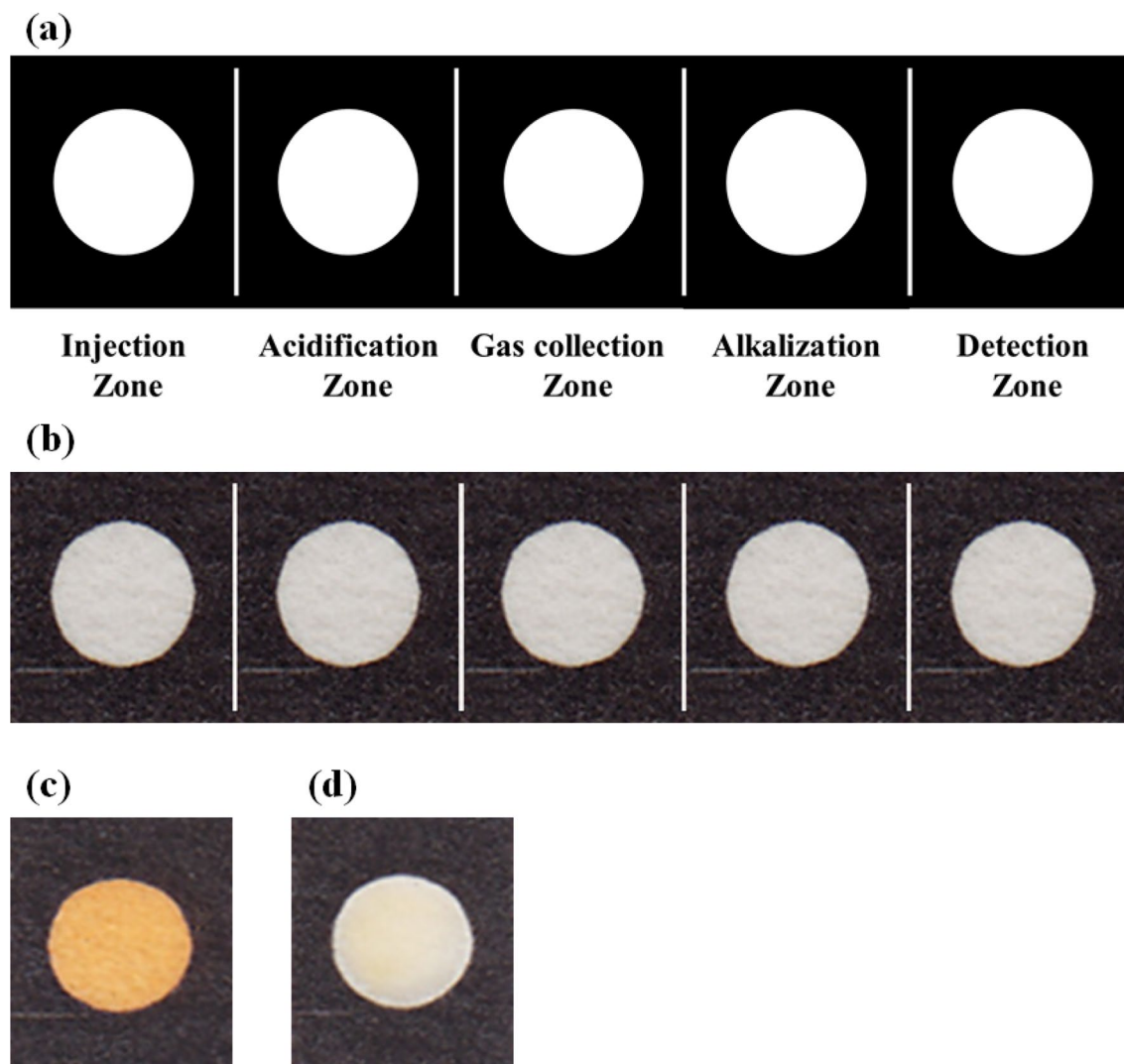


**Figure 1.** (a) The schematic pattern and (b) the image of fabricated  $\mu$ PAD, (c) the image of detection zone after injecting receptor, (d) the image of detection zone after exposing to  $100.0 \mu\text{mol L}^{-1}$  of cyanide ions.

To start the optimization, the experiment was performed by  $1.0 \mu\text{L}$  of TCA (15.0% W/V),  $1.0 \mu\text{L}$  of Tris buffer (0.1 M) and  $1.0 \mu\text{L}$  of the receptor ( $1.0 \text{ mg mL}^{-1}$ ).

In the first step, the effect of volume of analyte on the sensor response was investigated. As Fig. 2a shows, the best interaction occurred when  $2.0 \mu\text{L}$  of analyte was consumed. In other words, lower volumes are not enough for passing the sample to the detection zone, and the higher volumes washed the receptors to the side of detection zone and caused a large portion of the response to be lost. For further studies,  $2.0 \mu\text{L}$  of the sample was used.

TCA was employed to acidify the sample. The ability of this material for breaking the covalence bond between cyanide and protein depends on the concentration. Therefore, the mechanism of acidification was applied at different concentrations of TCA in the range of 5–45% W/V. As Fig. 2b shows, the best dissociation was observed at the concentration of 25% W/V. At higher values, no significant changes were observed in the assay responses. Therefore, 25% W/V was selected as the optimum concentration of TCA for further studies.

The gas produced in the previous step can be transferred to the next layer, immediately or during a specified interval. As Fig. 2c clearly shows, it is better to place a layer for gas collection between acidification and alkalization steps. Unlike the immediate transfer, this work helped the gas to have enough time for entering to the alkaline media, deprotonating and transforming to cyanide ions. Increase of the number of layers has no desirable effect on the response, since a portion of gas remained in the paper texture or its flow to the next step was slow, prolonging the time of analysis. Therefore, the device was fabricated by five layers.

To investigate the effect of type of buffer on the interaction of the cyanide and receptor, the examination was performed in both Tris and borate buffer (pH 11.0). As explained in Fig. 2d, borate buffer is an appropriate media for this interaction. Additionally, the concentration of buffer was evaluated in Fig. 2e. Obviously, the sensor response increases by increasing the buffer concentration up to 0.1 M. The higher concentration was not useful due to interfering of the ion-ion interaction<sup>36</sup>. To find the effective pH value for this interaction, the pH of buffer changed in the range of 7.0–12.0. The results were collected in Fig. 2f. As seen, the maximum response

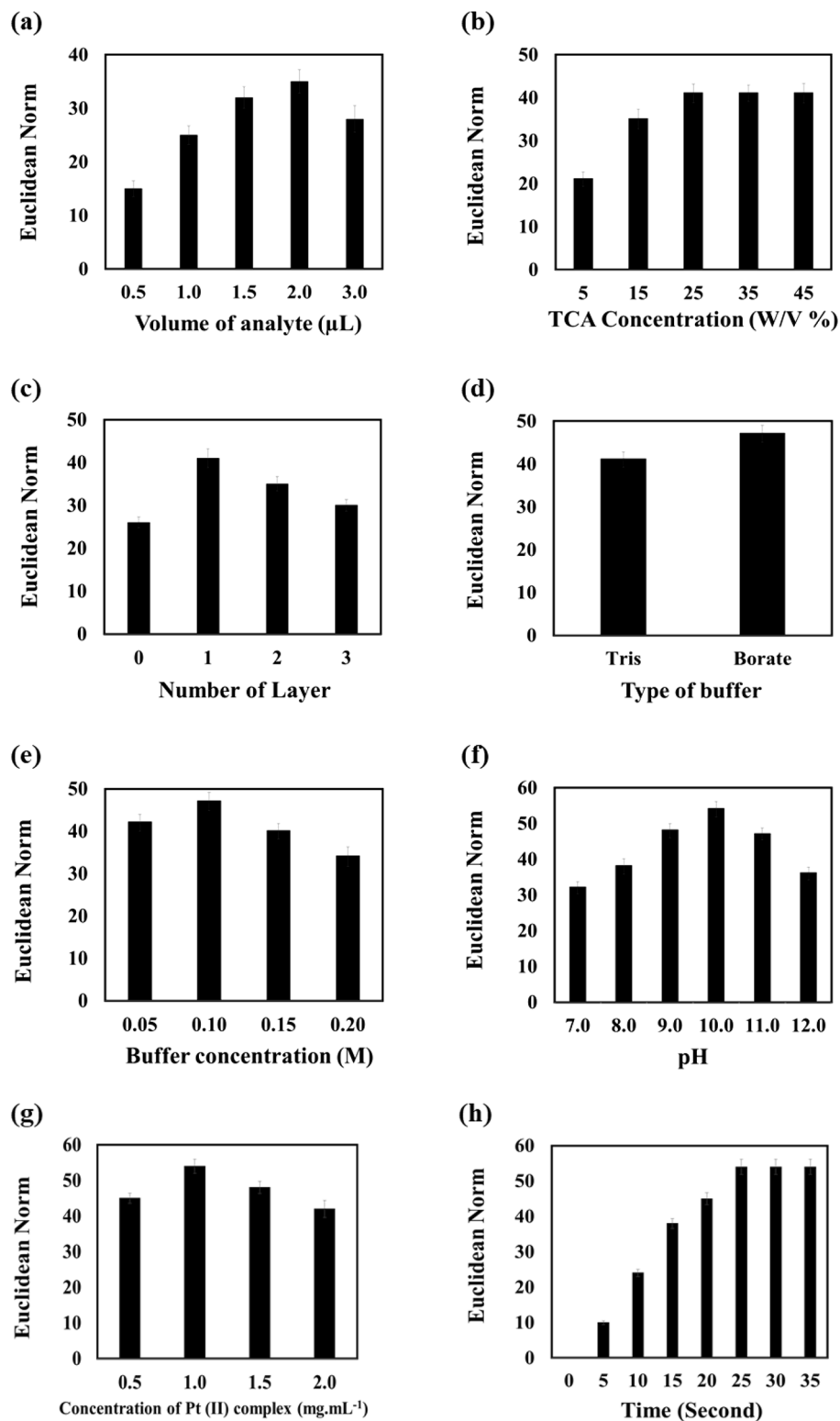


**Figure 2.** The effect of parameters including (a) volume of analyte, (b) TCA concentration, (c) number of gas collection layer, (d) type of buffer, (e) concentration of buffer, (f) pH of alkalization zone, (g) concentration of Pt (II) complex as receptor and (h) time of reaction on the response of sensor. The results were achieved in the presence of cyanide ions with the concentration of  $40.0 \mu\text{mol L}^{-1}$ .

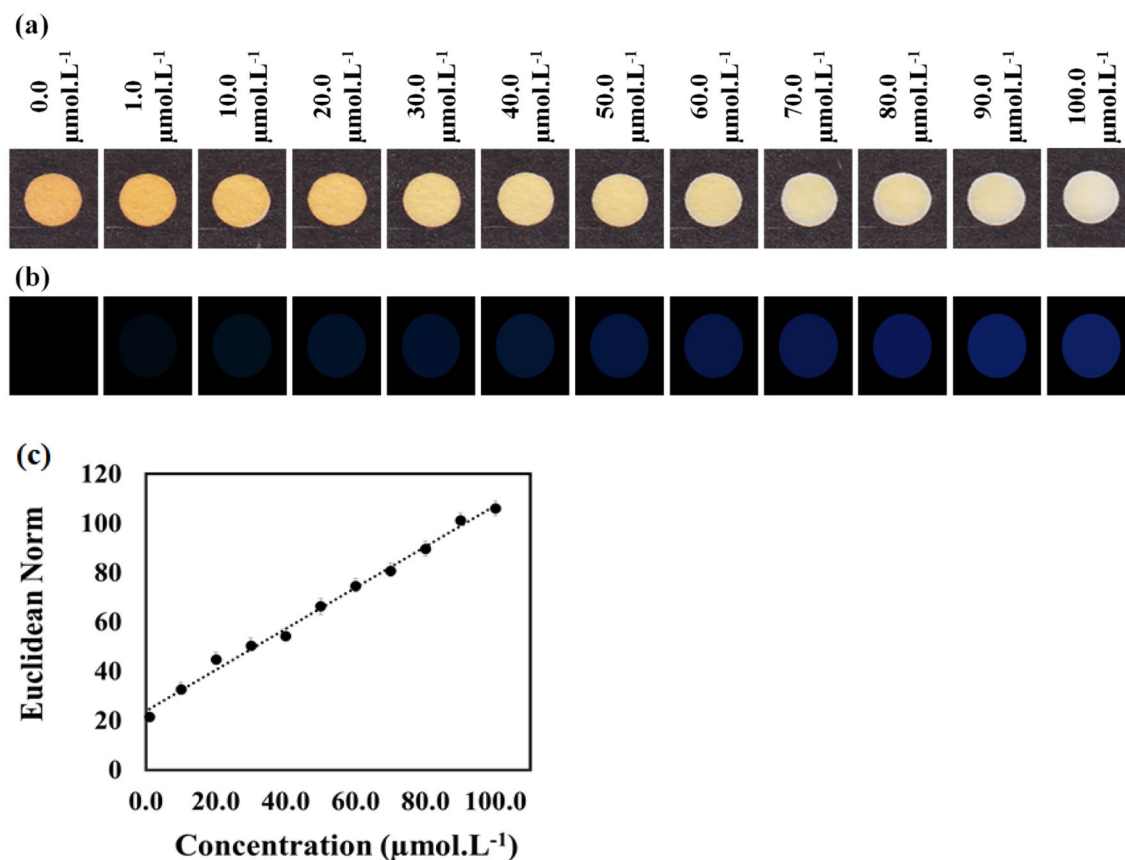


**Figure 3.** (a) The colorimetric responses, (b) the color difference maps and (c) the calibration curve for different concentration of cyanide ions. The study was performed in the presence of TCA (25.0% W/V), borate buffer (0.1 M, pH 10.0) and receptor (1.0 mg mL<sup>-1</sup>). 2.0  $\mu\text{L}$  of analyte was injected and the image of sensor was captured after 25 s.

was obtained at pH 10.0. At lower pH, cyanide existed in the protonated form (HCN), so that the response of the assay was decreased. The unsuitable result at higher pH is due to hydroxyl ions interferences<sup>36</sup>.

The receptor (Pt (II) complex) concentration can affect the performance of the assay. For this purpose, different amounts of the receptor in the range of (0.5–2.0 mg mL<sup>-1</sup>) were prepared to participate in interaction with cyanide ions. As Fig. 2g illustrates, 1.0 mg mL<sup>-1</sup> was a proper concentration. The complete interaction did not occur between cyanide and receptor at lower concentrations. Additionally, the intense color of the receptor at higher concentrations masked the partial differences caused by the interaction of the receptor and cyanide. Furthermore, the receptor with the concentration of 1.0 mg mL<sup>-1</sup> was used.

To find the optimum time, the incubation of the receptor and cyanide was monitored 0 to 40 s. As Fig. 2h shows, the appropriate time for flowing the sample through the layers of paper and having a complete interaction with receptors was 25 s. After that, the assay responses remained constant, and no color changes occurred. Therefore, the photos of the detection zone were collected after 25 s.

**Quantitative analysis.** The fabricated  $\mu\text{PAD}$  was applied to examine the different concentrations of cyanide in aqueous solutions. The amount of cyanide varied from 0 to 100.0  $\mu\text{mol L}^{-1}$ . Figure 3a shows the colorimetric responses. The yellow color of the receptor gradually faded by increasing the cyanide concentration. Figure 3b depicts the changes in the color of the receptor before and after exposure to analyte as colorimetric difference maps. As seen, the color intensity was amplified when the amount of cyanide was boosted to higher values. The pure responses for each concentration were calculated and used to plot the calibration curve. As Fig. 3c shows, the relationship between the sensor responses and cyanide concentrations was linear in the range of 1.0–100.0  $\mu\text{mol L}^{-1}$ . The limit of detection was obtained as 0.4  $\mu\text{mol L}^{-1}$ . Table 1 presents the list of the analytical performance of the proposed  $\mu\text{PAD}$ . The results reveal that  $\mu\text{PAD}$  was capable of determining cyanide ions with acceptable sensitivity and a wide dynamic range.

**Evaluation of reproducibility.** Five fabricated  $\mu\text{PAD}$ s were separately exposed to 40.0  $\mu\text{mol L}^{-1}$  of cyanide ions to investigate the reproducibility of assay responses. For each  $\mu\text{PAD}$ , the color intensities and the Euclidean norm of response vector were determined. As Fig. 4a,b respectively illustrates the colorimetric difference maps and the bar plot which are represented the same responses for five determinations. The relative standard error



Figures of merit	Value
Linear range ( $\mu\text{mol L}^{-1}$ )	1.0–100.0
Limit of detection ( $\mu\text{mol L}^{-1}$ )	0.4
Correlation coefficient	0.992
Calibration sensitivity	0.8
Analytical sensitivity (for $90.0 \mu\text{mol L}^{-1}$ )	0.3

**Table 1.** The analytical features L for determination of cyanide by using the proposed assay.

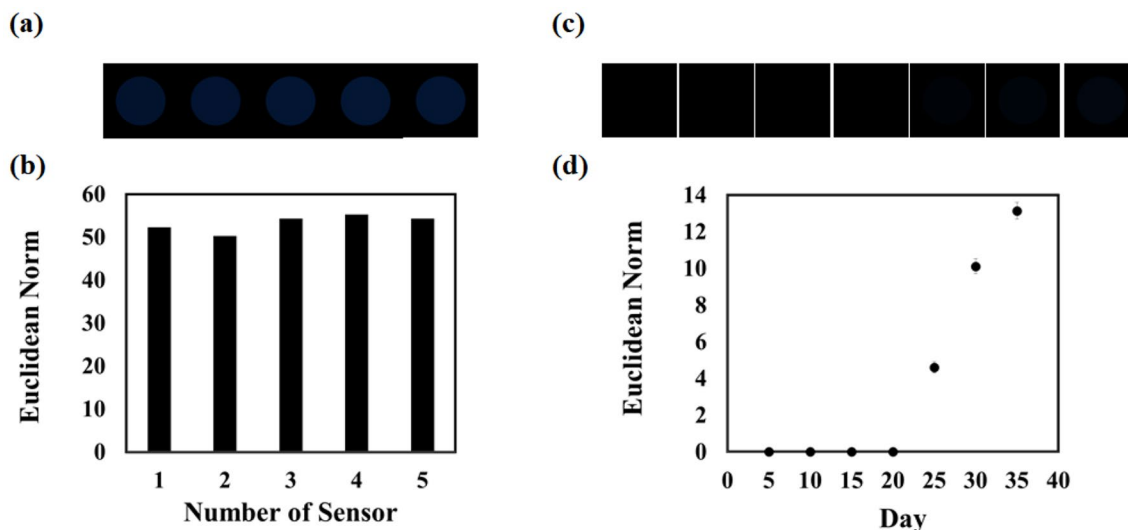


**Figure 4.** Evaluation of reproducibility of responses: (a) colorimetric difference maps and (b) numerical plot. Evaluation of the stability of fabricated  $\mu\text{PAD}$ : (c) colorimetric difference maps and (d) numerical plot. The study was performed in the presence of  $2.0 \mu\text{L}$  of analyte ( $40.0 \mu\text{mol L}^{-1}$ ), TCA (25.0% W/V), borate buffer ( $0.1 \text{ M}$ , pH 10.0) and receptor ( $1.0 \text{ mg mL}^{-1}$ ) and the image of sensor was captured after 25 s.

was equal to 3.77%, being lower than the tolerance value (5.0%). The result indicates that the proposed assay provide reproducible responses to cyanide ions with the identical concentration.

**Stability of sensor.** It is possible that the receptor will be degraded under different environmental conditions. Therefore, it is necessary to check how long the sensor is stable. For this purpose, the color intensity of the receptor was investigated for a period of time. As Fig. 4c,d shows, there were no changes in the color of the receptor for 20 days. After that, the receptor lost its durability against thermal and physicochemical variations. The cyanide ions were subjected to  $\mu\text{PAD}$  immediately and 20 days after the fabrication process. The results were compared to each other by statistical methods. As Table S2 illustrates, no significant difference was observed between the obtained responses. Therefore,  $\mu\text{PAD}$  can be stored at ambient air for 20 days before being used for analysis.

**Study of interferences.** To estimate the selectivity of assay responses,  $\mu\text{PAD}$  was employed to detect cyanide ions ( $40.0 \mu\text{mol mL}^{-1}$ ) in the presence of different interfering materials. The amount of foreign species was 100, 50 and 20 times higher than the cyanide concentration. For this study, the effects of a number of cations ( $\text{Na}^+$ ,  $\text{K}^+$ ,  $\text{Ca}^{2+}$ ,  $\text{Mg}^{2+}$ ,  $\text{Fe}^{3+}$ ,  $\text{Fe}^{2+}$ ,  $\text{Al}^{3+}$ ), anions ( $\text{NO}_3^-$ ,  $\text{PO}_4^{3-}$ ,  $\text{SO}_4^{2-}$ ,  $\text{CO}_3^{2-}$ ,  $\text{SO}_3^{2-}$ ,  $\text{Br}^-$ ,  $\text{Cl}^-$ ,  $\text{I}^-$ ,  $\text{SCN}^-$ ) and chemical and biological compounds (uric acid, urea, nicotine, ethanol, cholesterol, cysteine, glucose, urea) were evaluated. As Table 2 clearly shows, the assay was resistant to interfering species with the concentration at least 20 times more than cyanide concentrations. It shows that a robust complex was formed between the receptor and cyanide ions, thereby enhancing the selectivity of the proposed method for the studied analyte. On the other hands, the Euclidean norm as the response of sensor obtained for only cyanide ( $40.0 \mu\text{mol L}^{-1}$ ) was compared with those calculated for a mixture of cyanide and a certain foreign species which are mixing together with the ratio of (1:1). The results are represented in Figure S3. As shown, the presence of foreign species did not have any effects on the determination of cyanide.

**Real sample analysis.** The ability of the assay in detection and determination of cyanide ions in blood samples was verified. The experiment was performed with the help of normal people, firemen and fire victims. Since cigarette smoking can affect the amount of cyanide, both smokers and non-smokers participated in this

Foreign species	Tolerance <sup>1</sup> [Foreign species]/[Cyanide]
Na <sup>+</sup> , K <sup>+</sup> , Ca <sup>2+</sup> , Mg <sup>2+</sup> , Fe <sup>3+</sup> , Fe <sup>2+</sup> , Al <sup>3+</sup> , NO <sub>3</sub> <sup>-</sup> , PO <sub>4</sub> <sup>3-</sup> , SO <sub>4</sub> <sup>2-</sup> , CO <sub>3</sub> <sup>2-</sup> , Uric acid, Nicotine, Ethanol, Cholesterol, Cysteine, Glucose	500
Urea, SO <sub>3</sub> <sup>2-</sup> , Br <sup>-</sup> , Cl <sup>-</sup> , ClO <sup>-</sup>	50
I <sup>-</sup> , SCN <sup>-</sup>	20

**Table 2.** The effect of foreign species on the response of assay to cyanide ions (40.0  $\mu\text{mol L}^{-1}$ ). <sup>1</sup>The tolerance limit is introduced as the amount of foreign species in the presence of cyanide leading to a relative error less than 5% in the determination of cyanide.

Volunteer	Number of sample	Found <sup>1</sup> ( $\mu\text{mol/L}$ )		$t_{\text{experimental}}$ <sup>3</sup>	Relative error (%)
		Proposed sensor	GC/MS <sup>2</sup>		
Control (Non-Smoker)	1	2.5 ( $\pm 0.11$ )	2.6 ( $\pm 0.082$ )	1.30	- 3.8
	2	1.7 ( $\pm 0.063$ )	1.8 ( $\pm 0.050$ )	2.50	- 5.6
	3	1.3 ( $\pm 0.067$ )	1.2 ( $\pm 0.031$ )	1.82	8.3
	4	2.6 ( $\pm 0.12$ )	2.5 ( $\pm 0.088$ )	2.25	4.0
	5	2.1 ( $\pm 0.11$ )	2.2 ( $\pm 0.017$ )	1.61	- 4.5
Control (Smoker)	1	6.3 ( $\pm 0.32$ )	6.0 ( $\pm 0.22$ )	1.73	5.0
	2	7.1 ( $\pm 0.34$ )	6.7 ( $\pm 0.24$ )	2.15	6.0
	3	5.8 ( $\pm 0.30$ )	6.1 ( $\pm 0.26$ )	1.69	- 4.9
	4	6.5 ( $\pm 0.23$ )	6.3 ( $\pm 0.25$ )	1.32	3.2
	5	7.3 ( $\pm 0.30$ )	7.7 ( $\pm 0.34$ )	1.97	- 5.2
Firemen (non-smokers)	1	3.4 ( $\pm 0.16$ )	3.6 ( $\pm 0.12$ )	2.16	- 5.6
	2	2.9 ( $\pm 0.13$ )	3.1 ( $\pm 0.12$ )	2.53	- 6.4
	3	3.8 ( $\pm 0.20$ )	3.6 ( $\pm 0.15$ )	1.79	5.6
	4	3.6 ( $\pm 0.17$ )	3.4 ( $\pm 0.11$ )	2.21	5.9
	5	3.4 ( $\pm 0.18$ )	3.5 ( $\pm 0.15$ )	0.95	- 2.8
Firemen (smokers)	1	7.8 ( $\pm 0.33$ )	8.2 ( $\pm 0.31$ )	1.98	- 4.9
	2	9.6 ( $\pm 0.45$ )	9.1 ( $\pm 0.37$ )	1.92	5.5
	3	8.5 ( $\pm 0.41$ )	8.0 ( $\pm 0.28$ )	2.25	6.2
	4	10.2 ( $\pm 0.49$ )	9.8 ( $\pm 0.33$ )	1.51	- 4.1
	5	8.7 ( $\pm 0.35$ )	8.3 ( $\pm 0.26$ )	2.05	4.8
Non-fatal casualties	1	22.4 ( $\pm 1.01$ )	21.2 ( $\pm 0.67$ )	2.21	5.7
	2	30.2 ( $\pm 1.05$ )	28.4 ( $\pm 1.03$ )	2.73	6.3
	3	34.0 ( $\pm 1.53$ )	35.7 ( $\pm 1.31$ )	1.88	- 4.8
	4	19.5 ( $\pm 1.03$ )	20.8 ( $\pm 0.88$ )	2.14	- 6.2
	5	27.1 ( $\pm 1.28$ )	28.6 ( $\pm 0.82$ )	2.21	- 5.2
Fatal casualties	1	42.6 ( $\pm 2.24$ )	45.0 ( $\pm 1.64$ )	1.93	- 5.3
	2	69.4 ( $\pm 3.28$ )	65.7 ( $\pm 2.15$ )	2.11	5.6
	3	49.1 ( $\pm 1.99$ )	52.2 ( $\pm 1.50$ )	2.78	- 5.9
	4	55.0 ( $\pm 2.84$ )	51.7 ( $\pm 1.63$ )	2.25	6.4
	5	62.1 ( $\pm 2.70$ )	59.5 ( $\pm 1.82$ )	1.78	4.4

**Table 3.** Determination of cyanide concentration in the blood sample of fire survivors. <sup>1</sup>Mean of 5 determination ( $\pm$  SD). <sup>2</sup>Gas chromatography-Mass spectroscopy. <sup>3</sup> $t_{\text{critical}}$  (8, 0.05) = 2.31.

study. A sample of 5.0 ml was taken from each participant. Each sample was centrifuged at 5000 g for 7 min to separate the plasma section from the other parts of blood. Additionally, 1.0  $\mu\text{L}$  of the separated plasma was injected into  $\mu\text{PAD}$ . The parallel analysis was conducted by GC/MS as a reference method. The results obtained by both analytical techniques were presented in Table 3 and statistically compared to each other. As shown, the values of both relative error and  $t$  student test were lower than the critical values. It confirmed a good correlation between the results of the developed assay and the reference technique. Therefore, the fabricated  $\mu\text{PAD}$  can be a reliable alternative to cyanide measurements in biological samples. As Table 3 shows, the mean of the cyanide concentration in different studied categories were acquired as 2.0, 6.6, 3.4, 9.0, 26.6 and 55.6  $\mu\text{mol L}^{-1}$  for control (non-smoker), control (smoker), firemen (non-smokers), firemen (smokers), non-fatal casualties and fatal casualties, respectively. Based on the mean values, the amount of cyanide in the people who were dead was higher than 20.0  $\mu\text{mol L}^{-1}$ . As observed, the cyanide concentration is higher in firemen than in control samples (who

were not exposed to fire smoke); however, it is much less than the quantities of cyanide in fire victims. Compared to non-smokers, the level of cyanide was increased in smoker volunteers.

The analytical characterizations of the fabricated  $\mu$ PAD were compared to a number of colorimetric sensors to determine cyanide. The published methods used various receptors such as metal complex, bimetallic nanoparticles and organic materials. Thus, the Pt complex has not been used as a colorimetric detector of cyanide ions up to now. As Table S3 shows, the proposed assay shows a good linear range and low-level detection limit compared to the previous methods. Also, the fabricated sensor consumed only 2.0  $\mu$ L of analyte and detected cyanide in the shortest possible time rather than the other methods.

## Conclusion

This study introduced a simple colorimetric assay using a square-planar platinum (II) complex as a receptor of cyanide ions. The assay was prepared based on the origami art assembling all experimental steps in a piece of paper, used a trace volume of analyte and consumed a few seconds for analysis. These advantages cause  $\mu$ PAD to have better performance than ordinary instrumental methods and other paper-based devices. The receptor showed high affinity to cyanide ions in the presence of other co-existing compounds. The response of sensor has a linear correlation with the cyanide concentrations in the range of 1.0–100.0  $\mu\text{mol L}^{-1}$ . The detection limit was calculated as 0.4  $\mu\text{mol L}^{-1}$  for this determination. The calibration and analytical sensitivity were equal to 0.8 and 0.3. The proposed  $\mu$ PAD opens a new way to determine the amount of cyanide in water, food and blood samples, being important for both forensic and medical centers to explore the reasons for human death or his suicide.

## Methods

All methods were performed in accordance with the relevant guidelines and regulations.

**Chemicals and materials.** All chemical compounds were used in analytical grades without any purifications. Some materials such as potassium nitrate ( $\text{KNO}_3$ ), potassium cyanide (KCN), sodium nitrate ( $\text{NaNO}_3$ ), sodium nitrite ( $\text{NaNO}_2$ ), sodium carbonate ( $\text{Na}_2\text{CO}_3$ ), sodium sulfate ( $\text{Na}_2\text{SO}_4$ ), sodium sulfite ( $\text{Na}_2\text{SO}_3$ ), sodium phosphate ( $\text{Na}_3\text{PO}_4$ ), sodium thiocyanate ( $\text{NaSCN}$ ), sodium chloride (NaCl), sodium bromide (NaBr), sodium iodide (NaI), sodium hydroxide (NaOH), calcium nitrate tetrahydrate ( $\text{Ca}(\text{NO}_3)_2 \cdot 4\text{H}_2\text{O}$ ), magnesium nitrate hexahydrate ( $\text{Mg}(\text{NO}_3)_2 \cdot 6\text{H}_2\text{O}$ ), aluminium nitrate nonahydrate ( $\text{Al}(\text{NO}_3)_3 \cdot 9\text{H}_2\text{O}$ ), iron (II) sulfate heptahydrate ( $\text{FeSO}_4 \cdot 7\text{H}_2\text{O}$ ), iron (III) chloride hexahydrate ( $\text{FeCl}_3 \cdot 6\text{H}_2\text{O}$ ), ethanol, boric acid ( $\text{H}_3\text{BO}_3$ ), hydrochloric acid (HCl), tris-hydroxymethyl methane (Tris), acetone, n-hexane, 1,10-phenanthroline, cysteine, urea, uric acid, cholesterol, glucose, nicotine and trichloroacetic acid (TCA) were purchased from Merck Chemical Company.  $\mu$ PAD was fabricated by Whatman Grade NO.2 filter paper. The stock solution of cyanide ions was prepared with the concentration of 150.0  $\mu\text{mol L}^{-1}$ . Tris and borate buffer were made at the concentration of 0.2 M, and their pH was adjusted at an optimum value using NaOH (1.0 M) and HCl (1.0 M).

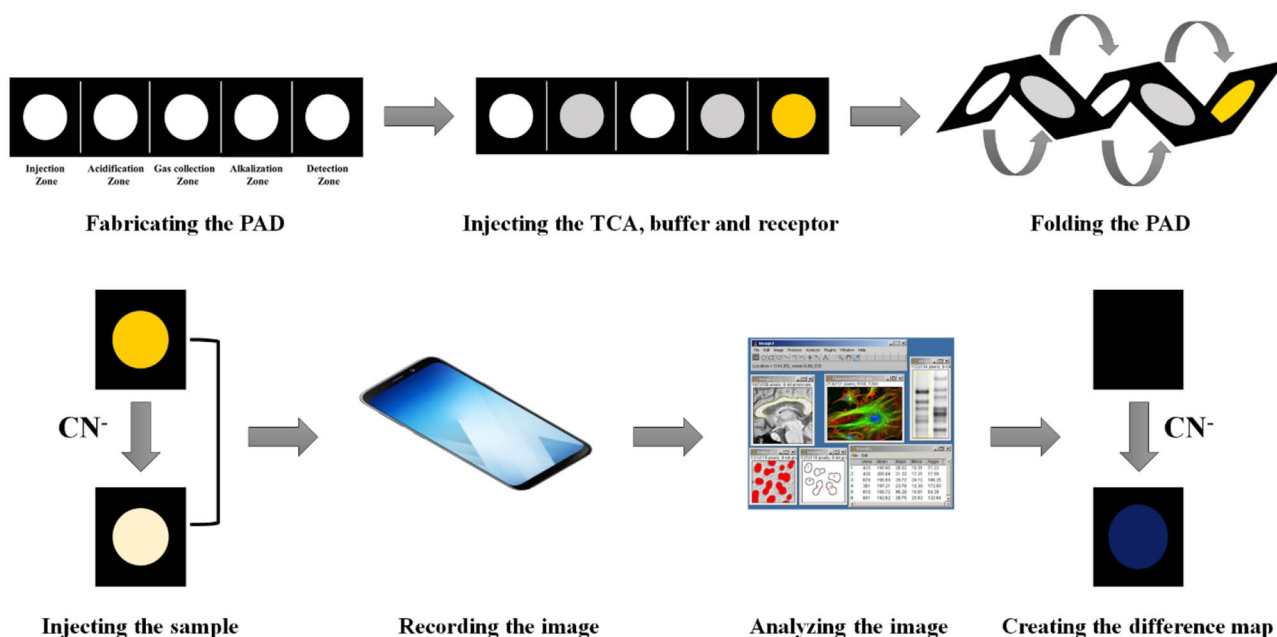
**Apparatus and software.** UV/Vis spectrophotometer (JASCO, Model V-570) and field emission scanning electron microscopy (FE-SEM; MIRA3 TESCAN) were used to characterize the paper device. Brand type micropipettes were employed for injection of samples. The pH of media was adjusted by a Metrohm 632 pH-meter (Model 780 pH lab). The schematic pattern of  $\mu$ PAD was drawn by the AutoCAD 2016 software (<https://www.autodesk.com/products/autocad>). A HP Laser Jet printer 1320 w was performed for printing pattern utilized to print patterns on the paper. The printer was equipped by a HP Q5949A toner cartridge with a resolution of 600 dpi. An oven (MEMMERT UN 30) was used to bake the paper. The sensor photographs were recorded by a smartphone (Samsung Galaxy A7). The image analysis was conducted by the Image J software (1.51n, National Institutes of Health, USA) (<https://imagej.nih.gov/ij/download.html>) and MATLAB R2015 scientific software (<https://www.mathworks.com>).

**Synthesis of receptor.** [Pt (*p*-MeC<sub>6</sub>H<sub>4</sub>)<sub>2</sub>(phen)] (Compound A) was used as a colorimetric sensing element in this study. The synthesis procedure and characterization of recognition element are described in the supporting information document (Sect. 2).

**$\mu$ PAD preparation.** Figure 1a shows the pattern designed by the AutoCAD software. It is a rectangle with a dimension of 1  $\times$  5 cm and made of two parts, including circle shaped hydrophilic zones (white sections) and a hydrophobic barrier (black section). The diameter of each circle was equal to 0.7 cm. Five zones are embedded in this pattern, which are distinct from each other using a line. Each zone is drawn for a specified task consisting of sample injection, sample acidification, gas collection, gas alkalization and analyte detection. The pattern is printed on a Whatman filter paper and then baked in the oven at 180  $^\circ\text{C}$  for 45 min<sup>37</sup>. Through this process, the printer ink is immobilized on the paper surface, and then melt and penetrated in the paper texture<sup>38</sup>. This work is performed to create a barrier with high hydrophobicity around the hydrophilic zones. Figure 1b presents the image of the fabricated  $\mu$ PAD.

**Colorimetric determination.** Each hydrophilic zone was filled by respective reagent: acidification zone was poured by TCA (25.0% W/V), borate buffer (0.1 M, pH 10.0) was added to the alkalization zone and finally, the Pt complex as a receptor was injected into the detection zone. Each zone contained 1.0  $\mu\text{L}$  of reagent. Furthermore, the gas collection zone was empty at this time. The  $\mu$ PAD was folded from the marked lines such that injection and detection zones were the top and bottom layers of the device, respectively. A paper holder was used to make the layers fit perfectly together. This holder is two layers of wood fastened together by a peg. There is a





**Scheme 1.** Summary of the experimental procedure for detection of cyanide ions.

hole in the top layer for injecting the samples. Moreover, 2.0  $\mu\text{L}$  of the cyanide containing sample was subjected to  $\mu\text{PAD}$  from the injection zone. The sample flowed through the layers of  $\mu\text{PAD}$  and reached the detection zone. It interacted with the receptor and changed the color of the receptor from yellow to being colorless. This interaction can be influenced by TCA concentration, pH of media, type of buffer and its concentration, amount of receptor, volume of sample and time required for interaction. Therefore, these parameters need to be optimized.

**Image analysis.** Changes in the color of the detection zone were monitored by a smartphone. To remove the effect of ambient light, the experiment was performed in a laboratory-made box containing two lamps (8 W). This box is a wooden cube with dimensions of 30 cm. The lamps are placed on the roof of this box such that they have a 45 degree angle with the location of the sample. The image of the sensor before and after exposure to analyte was recorded and saved with the name of “reference” and “response” images. Each image was uploaded to the Image J software. The whole area of the detection zone was selected. The software determined the intensities of R and G and B for pixel by pixel and finally the average of these intensities were calculated for each color elements. The difference between the color values of reference and response images was determined. For each analysis, three color values related to red, green and blue color elements were collected in a data vector. The Euclidean norm of the response vector was calculated as the pure response for further study:

$$\text{Euclidean norm} = \sqrt{(\Delta R)^2 + (\Delta G)^2 + (\Delta B)^2}$$

where  $\Delta R$ ,  $\Delta G$  and  $\Delta B$  are the difference color values for red, green and blue elements. Scheme 1 depicts the schematic diagram for the general process of detection.

The data vector containing the numerical color elements of R, G and B was converted to color circle shape with the help of image processing method in the MATLAB software.

**Determination of blood cyanide concentration.** *Use of human participants.* Identifying information. The participants were divided into six groups, including healthy people as control samples (smokers and non-smokers), firemen (smokers and non-smokers), non-fatal casualties and fatal casualties. The individuals were asked to read the proposal and filled the consent form. The informed consent was obtained. This form contains the definition of study, its cost, advantages, limitations and sampling procedures. In this form, we stated the personal information and medical documents for each participant would be kept confidential. Also, each person could refuse to participate in this study or leave the test at any time. The proposal for this study was approved by the Medical Ethics Committee of Ahvaz University of Medical Sciences (Ethics code: IR.AJUMS.REC.1398.337). In this proposal, all methods including fabrication of sensor, detection procedure, statistical and confirmation analysis was completely explained.

**Experimental procedure.** The  $\mu\text{PAD}$  was applied to determine the amount of cyanide ions in blood sample. The volunteers were selected from fire victims and healthy peoples. Furthermore, the effect of smoking on BCC was investigated. They were given us their blood samples collected in a sterile tubes. To prevent the blood clotting, it was mixed with heparin. The plasma portion of blood was separated and used for further studies. The plasma samples were partitioned in two identical parts: half of sample was analyzed by GC/MS, and the rest was

examined by the fabricated  $\mu$ PAD. In our study, the experiment was performed as it was conducted in the previous section. The results obtained by the colorimetric method were compared to those achieved by the standard assay with the help of statistical parameters.

Received: 15 November 2020; Accepted: 29 January 2021

Published online: 10 February 2021

## References

- Lindsay, A. E., Greenbaum, A. R. & O'Hare, D. Analytical techniques for cyanide in blood and published blood cyanide concentrations from healthy subjects and fire victims. *Anal. Chim. Acta* **511**, 185–195 (2004).
- Tian, Y. *et al.* A disposable blood cyanide sensor. *Anal. Chim. Acta* **768**, 129–135 (2013).
- Stoll, S., Roeder, G. & Keil, W. Concentrations of cyanide in blood samples of corpses after smoke inhalation of varying origin. *Int. J. Legal Med.* **131**, 123–129 (2017).
- Yu, J. C. C. & Mozayani, A. Medicolegal and forensic factors in cyanide poisoning. *Toxicol. Cyanides Cyanogens Exp. Appl. Clin. Asp.* **2016**, 276–282. <https://doi.org/10.1002/9781118628966.ch20> (2016).
- Kaita, Y., Tarui, T., Shoji, T., Miyauchi, H. & Yamaguchi, Y. Cyanide poisoning is a possible cause of cardiac arrest among fire victims, and empiric antidote treatment may improve outcomes. *Am. J. Emerg. Med.* **36**, 851–853 (2018).
- Yáñez-Sedeño, P., Agüí, L., Villalonga, R. & Pingarrón, J. M. Biosensors in forensic analysis. A review. *Anal. Chim. Acta* **823**, 1–19 (2014).
- Jackson, R. & Logue, B. A. A review of rapid and field-portable analytical techniques for the diagnosis of cyanide exposure. *Anal. Chim. Acta* **960**, 18–39 (2017).
- Randviir, E. P. & Banks, C. E. The latest developments in quantifying cyanide and hydrogen cyanide. *TrAC Trends Anal. Chem.* **64**, 75–85 (2015).
- Ma, J. & Dasgupta, P. K. Recent developments in cyanide detection: a review. *Anal. Chim. Acta* **673**, 117–125 (2010).
- Xu, Z., Chen, X., Kim, H. N. & Yoon, J. Sensors for the optical detection of cyanide ion. *Chem. Soc. Rev.* **39**, 127–137 (2010).
- Wang, F., Wang, L., Chen, X. & Yoon, J. Recent progress in the development of fluorometric and colorimetric chemosensors for detection of cyanide ions. *Chem. Soc. Rev.* **43**, 4312–4324 (2014).
- Udhayakumari, D. Chromogenic and fluorogenic chemosensors for lethal cyanide ion. A comprehensive review of the year 2016. *Sens. Actuat. B Chem.* **259**, 1022–1057 (2018).
- Khajehsharif, H. & Sheini, A. A selective naked-eye detection and determination of cysteine using an indicator-displacement assay in urine sample. *Sens. Actuat. B Chem.* **199**, 457–462 (2014).
- Khajehsharif, H. & Bordbar, M. M. A highly selective chemosensor for detection and determination of cyanide by using an indicator displacement assay and PC-ANN and its logic gate behavior. *Sens. Actuat. B Chem.* **209**, 1015–1022 (2015).
- Yoon, H., Lee, C. H., Jeong, Y. H., Gee, H. C. & Jang, W. D. A zinc porphyrin-based molecular probe for the determination of contamination in commercial acetonitrile. *Chem. Commun.* **48**, 5109–5111 (2012).
- Lee, J. H., Reum Jeong, A., Shin, I. S., Kim, H. J. & Hong, J. I. Fluorescence turn-on sensor for cyanide based on a cobalt(II)-coumarinylsalen complex. *Org. Lett.* **12**, 764–767 (2010).
- Jung, H. S., Han, J. H., Kim, Z. H., Kang, C. & Kim, J. S. Coumarin-Cu(II) ensemble-based cyanide sensing chemodosimeter. *Org. Lett.* **13**, 5056–5059 (2011).
- Tang, L. & Cai, M. A highly selective and sensitive fluorescent sensor for Cu<sup>2+</sup> and its complex for successive sensing of cyanide via Cu<sup>2+</sup> displacement approach. *Sens. Actuat. B Chem.* **173**, 862–867 (2012).
- Tetilla, M. A. *et al.* Colorimetric response to anions by a “robust” copper(II) complex of a [9]aneN<sub>3</sub> pendant arm derivative: CN<sup>-</sup> and I<sup>-</sup> selective sensing. *Chem. Commun.* **47**, 3805–3807 (2011).
- Zou, Q. *et al.* Unsymmetrical diarylethenes as molecular keypad locks with tunable photochromism and fluorescence via Cu<sup>2+</sup> and CN<sup>-</sup> coordinations. *Chem. Commun.* **48**, 2095–2097 (2012).
- Yu, C., Wong, K. M. C., Chan, K. H. Y. & Yam, V. W. W. Polymer-induced self-assembly of alkynylplatinum(II) terpyridyl complexes by metal $\cdots$ metal/ $\pi\cdots\pi$  interactions. *Angew. Chemie Int. Ed.* **44**, 791–794 (2005).
- Yam, V. W. W., Chan, K. H. Y., Wong, K. M. C. & Zhu, N. Luminescent platinum(II) terpyridyl complexes: Effect of counter ions on solvent-induced aggregation and color changes. *Chem. A Eur. J.* **11**, 4535–4543 (2005).
- Tam, A. Y. Y., Wong, K. M. C., Wang, G. & Yam, V. W. W. Luminescent metallogels of platinum(II) terpyridyl complexes: Interplay of metal $\cdots$ metal,  $\pi\cdots\pi$  and hydrophobic-hydrophobic interactions on gel formation. *Chem. Commun.* <https://doi.org/10.1039/b705062c> (2007).
- Demas, J. N. & DeGraff, B. A. Applications of luminescent transition platinum group metal complexes to sensor technology and molecular probes. *Coord. Chem. Rev.* **211**, 317–351 (2001).
- Shaik, K. & Petersen, J. An investigation of the leaching of Pt and Pd from cooperite, sperrylite and column bioleached concentrates in thiocyanate-cyanide systems. *Hydrometallurgy* **173**, 210–217 (2017).
- Martinez, A. W., Phillips, S. T., Whitesides, G. M. & Carrilho, E. Diagnostics for the developing world: microfluidic paper-based analytical devices. *Anal. Chem.* **82**, 3–10 (2010).
- Bordbar, M. M., Barzegar, H., Tashkhourian, J., Bordbar, M. & Hemmateenejad, B. A non-invasive tool for early detection of acute leukemia in children using a paper-based optoelectronic nose based on an array of metallic nanoparticles. *Anal. Chim. Acta* **1141**, 28–35 (2021).
- Sheini, A. A point-of-care testing sensor based on fluorescent nanoclusters for rapid detection of septicemia in children. *Sens. Actuat. B Chem.* <https://doi.org/10.1016/j.snb.2020.129029> (2020).
- Xia, Y., Si, J. & Li, Z. Fabrication techniques for microfluidic paper-based analytical devices and their applications for biological testing: a review. *Biosens. Bioelectron.* **77**, 774–789 (2016).
- Sheini, A. A paper-based device for the colorimetric determination of ammonia and carbon dioxide using thiomalic acid and maltol functionalized silver nanoparticles: application to the enzymatic determination of urea in saliva and blood. *Microchim. Acta* **187** (2020).
- Bordbar, M. M., Nguyen, T. A., Tran, A. Q. & Bagheri, H. Optoelectronic nose based on an origami paper sensor for selective detection of pesticide aerosols. *Sci. Rep.* **10** (2020).
- Bordbar, M. M., Nguyen, T. A., Arduini, F. & Bagheri, H. A paper-based colorimetric sensor array for discrimination and simultaneous determination of organophosphate and carbamate pesticides in tap water, apple juice, and rice. *Microchim. Acta* **187** (2020).
- Morbioli, G. G., Mazzu-Nascimento, T., Stockton, A. M. & Carrilho, E. Technical aspects and challenges of colorimetric detection with microfluidic paper-based analytical devices ( $\mu$ PADs)—a review. *Anal. Chim. Acta* **970**, 1–22 (2017).
- Petruci, J. F. S., Hauser, P. C. & Cardoso, A. A. Colorimetric paper-based device for gaseous hydrogen cyanide quantification based on absorbance measurements. *Sens. Actuat. B Chem.* **268**, 392–397 (2018).

35. Chaudhary, M. T. *et al.* Rapid and economical colorimetric detection of cyanide in blood using vitamin B12. *Aust. J. Forensic Sci.* **48**, 42–49 (2016).
36. Bordbar, M. M., Hemmateenejad, B., Tashkhourian, J. & Nami-Ana, S. F. An optoelectronic tongue based on an array of gold and silver nanoparticles for analysis of natural, synthetic and biological antioxidants. *Microchim. Acta* **185** (2018).
37. Carrilho, E., Martinez, A. W. & Whitesides, G. M. Understanding wax printing: a simple micropatterning process for paper-based microfluidics. *Anal. Chem.* **81**, 7091–7095 (2009).
38. Sheini, A. Colorimetric aggregation assay based on array of gold and silver nanoparticles for simultaneous analysis of aflatoxins, ochratoxin and zearalenone by using chemometric analysis and paper based analytical devices. *Microchim. Acta* **187** (2020).

## Acknowledgements

The authors gratefully acknowledge from the Research Councils of Shohadaye Hoveizeh University of Technology and Ahvaz Jundishapur University of Medical Sciences.

## Author contributions

A.S. conceived the idea, designed and discussed the concepts and experiments, and analyzed the data. M.D.A. synthesized the receptor, designed and discussed the concepts and experiments. M.M.B. performed the experimental work and analyzed the data. All authors discussed and commented on the manuscript.

## Competing interests

The authors declare no competing interests.

## Additional information

**Supplementary Information** The online version contains supplementary material available at <https://doi.org/10.1038/s41598-021-83186-0>.

**Correspondence** and requests for materials should be addressed to A.S.

**Reprints and permissions information** is available at [www.nature.com/reprints](http://www.nature.com/reprints).

**Publisher's note** Springer Nature remains neutral with regard to jurisdictional claims in published maps and institutional affiliations.



**Open Access** This article is licensed under a Creative Commons Attribution 4.0 International License, which permits use, sharing, adaptation, distribution and reproduction in any medium or format, as long as you give appropriate credit to the original author(s) and the source, provide a link to the Creative Commons licence, and indicate if changes were made. The images or other third party material in this article are included in the article's Creative Commons licence, unless indicated otherwise in a credit line to the material. If material is not included in the article's Creative Commons licence and your intended use is not permitted by statutory regulation or exceeds the permitted use, you will need to obtain permission directly from the copyright holder. To view a copy of this licence, visit <http://creativecommons.org/licenses/by/4.0/>.

© The Author(s) 2021